



Research article

PSTi8 with metformin ameliorates perimenopause induced steatohepatitis associated ER stress by regulating SIRT-1/SREBP-1c axis



Pragati Singh^a, Mohammad Irshad Reza^a, Anees A. Syed^{a,c}, Richa Garg^{a,c}, Athar Husain^{a,c}, Roshan Katekar^{a,c}, Umesh K. Goand^{a,c}, Mohammed Riyazuddin^a, Anand P. Gupta^a, Jiaur R. Gayen^{a,b,c,*}

^a *Pharmaceutics & Pharmacokinetics Division, CSIR-Central Drug Research Institute, Lucknow, 226031, India*

^b *Pharmacology Division, CSIR-Central Drug Research Institute, Lucknow 226031, India*

^c *Academy of Scientific and Innovative Research (AcSIR), Ghaziabad 201002, India*

ARTICLE INFO

Keywords:

Combination therapy (Met + PSTi8)

PSTi8

Metformin

Hepatic steatosis

ER stress

SIRT-1

SREBP-1c

Perimenopausal rat

ABSTRACT

Aims: Hepatic steatosis in women confronting menopause is the manifestation of substantial fructose consumption and forms a positive feedback loop to develop endoplasmic reticulum (ER) stress. Previously pancreastatin inhibitor peptide-8 (PSTi8) and Metformin (Met) combination effectively ameliorated hepatic lipid accumulation in high fructose diet (HFrD) fed diabetic mice models at reduced doses. Moreover, SIRT-1 plays a crucial role in the regulation of SREBP-1c. Hence we hypothesized that Met and PSTi8 in combination (at therapeutic lower doses) could mitigate hepatic steatosis linked ER stress by activating SIRT-1 and precluding SREBP-1c in HFrD fed 4-Vinylcyclohexenediepoxyde (HVCD) induced perimenopausal rats.

Main methods: HVCD rats were fed HFrD for 12 weeks, accompanied by 14 days of treatment with Met, PSTi8, and combination. We confirmed model establishment by estrus cycle study, estradiol level, and intraperitoneal glucose tolerance test. Plasma lipid profile and liver function were determined. Also, mRNA and protein expressions were examined. Moreover, distribution of SIRT-1 and SREBP-1c was detected in HepG2 cells by immunofluorescence staining.

Key findings: HVCD group displayed augmented insulin resistance (IR), lipogenesis, and ER stress in the liver. Combination therapy improved the estrus cyclicity, estradiol, and lipid profile of HVCD rats. Met and PSTi8 combination reduced hepatic SREBP-1c and triggered SIRT-1 expression in high fructose-induced insulin-resistant HepG2 cells; consequently, combination therapy attenuated ER stress.

Significance: Succinctly, present research promotes impetus concerning the remedial impact of Met with PSTi8 at lower therapeutic doses to ameliorate hepatic IR, steatosis, and associated ER stress by revamping the SIRT-1/SREBP-1c axis in perimenopausal rats.

1. Introduction

Endoplasmic reticulum (ER), a site for protein folding and calcium storage, is involved in the biosynthesis of macromolecules such as carbohydrates, lipids, and steroids [1]. ER homeostasis is impaired in response to increased physiological needs impacting its protein folding capacity, therefore promoting ER stress [2]. Liver cells are enriched in the ER due to the immense demand for protein synthesis and folding. Hepatocytes are vulnerable to perturbations in ER functioning and the development of ER stress [3]. ER orchestrates an adaptive unfolded protein response (UPR) to increase the fidelity of ER folding capacity

during mild ER stress [4]. Additionally, it has been suggested that ER stress is associated with altered hepatic lipid metabolism [5, 6]. Besides, the UPR pathway involving protein kinase PKR like ER kinase (PERK)/eukaryotic initiation factor-2 (eIF2 α)/ATF4 axis is essential for the expression of lipogenic genes [7, 8].

Insulin resistance (IR) arises in response to the activation of UPR in ER stress conditions [9]. It has been reported that hepatic steatosis is explicitly correlated with IR [10]. Moreover, the p-PERK-p-eIF2 α mediated UPR also drives IR [11] during ER stress. Furthermore, Sirtuin-1 (SIRT-1) is a master protein regulating glucose and lipid metabolism in response to nutrient availability [12, 13]. Liver-specific SIRT-1 knockout

* Corresponding author.

E-mail address: jr.gayen@cdri.res.in (J.R. Gayen).

<https://doi.org/10.1016/j.heliyon.2020.e05826>

Received 21 October 2020; Received in revised form 23 November 2020; Accepted 18 December 2020

2405-8440/© 2020 The Author(s). Published by Elsevier Ltd. This is an open access article under the CC BY-NC-ND license (<http://creativecommons.org/licenses/by-nc-nd/4.0/>).

rodents displayed hepatic steatosis [14]. Additionally, SIRT-1 has been reported to protect the heart from ER stress by modulating the PERK-eIF2 α -ATF4 arm of UPR [15]. Consistently, SIRT-1 regulates sterol response element-binding protein-1C (SREBP-1C) and other lipogenic gene expressions in liver [16].

Metformin (Met) is the first-line therapy for the treatment of type 2 diabetes and is considered a potent activator of SIRT-1 [17]. Met prevents hepatic fat accumulation by attenuating the expression of key regulators of lipogenesis such as SREBP-1C, fatty acid synthase (FAS), acetyl-CoA carboxylase (ACC) [18]. Additionally, Met inhibited ER stress by inhibiting p38MAPK signaling in ovarian granulosa cells [19].

Pancreastatin (PST) is an endogenous peptide that interacts with glucose-regulated protein (GRP78), which plays an influential role in regulating ER stress [20]. PST levels has been demonstrated to be increased by high fructose feeding in mice [21]. We previously unravelled Pancreastatin inhibitor peptide-8 (PSTi8, PEGKGEQHSQQKEEEEEMAV-amide), an inhibitor of PST. It was evinced that PSTi8 inhibits PST [20]; consequently, it may regulate GRP78 activity during ER stress, which remains unexplored.

It has been observed that excess dietary fat alone is insufficient to cause diet-induced obesity and IR [22] in female rodents. Herein, we have utilized an occupational compound 4-Vinylcyclohexenediepoxyde (VCD) to induce ovarian malfunctioning in female rats during high fructose feeding to achieve an efficient insulin-resistant model with impaired hepatic lipid metabolism, which may stimulate ER stress progression and chronic UPR. There are no existing targeted pharmacological alternatives for the treatment of hepatosteatosis. Hence there is an urgent need for specific pharmacological treatment to restrict liver steatosis development and associated comorbidities. Moreover, Met and PSTi8, in combination, may eliminate the paucity of potential therapeutic targets by working through different mechanisms and provide considerable background for the rational combination therapy of these agents. Additionally, Met and PSTi8 at the lower therapeutic doses previously ameliorated lipid accumulation in the liver of the high-fat diet fed diabetic mice model [23]. Therefore, we hypothesized that combination therapy of Met and PSTi8 in combination at lower therapeutic doses might ameliorate hepatic steatosis associated ER stress and UPR through the SIRT-1/SREBP-1c axis in high fructose diet (HFrD) fed/VCD-induced perimenopausal rats.

2. Materials & methods

2.1. Materials

PSTi8 peptide (PEGKGEQHSQQKEEEEEMAV-amide) has been designed by our research group, synthesized and purified by Life Tein LLC, USA. We obtained 1,1-Dimethylbiguanide HCl (Metformin) from Alfa Aesar. We purchased Dulbecco's modified eagle medium (DMEM), trypsin-EDTA, antibiotic-antimycotics, TRIzol, phosphate-buffered saline, stain Oil Red O and Nile Red were purchased from Sigma Aldrich, St. Louis, USA. We purchased high capacity cDNA reverse transcription kit, glucose/glucose oxidase assay kit (amplicon™ red), SYBR Green qPCR Kit (DyNAmo Color Flash), Immobilon Chemiluminescent HRP substrate by Thermo Fisher Scientific, Waltham, USA. RT-qPCR primers were purchased from Eurofins Scientific, Luxembourg. HFrD (calories (60%) from fructose, cat. No. D00111301) was obtained from research diets, Inc, USA. San Diego, USA. Primary antibody GRP78 (ab78432) was purchased from Abcam 1 Kendall Square, Suite B2304. Cambridge, MA. Antibodies p-AKT (4058S), pan AKT (4691S), p-IRS (2381P), IRS-1 (2382S) secondary antibody anti-mouse IgG (7076S) were purchased from Cell Signalling Technology, Denver. SREBP-1c (AF6283), SIRT-1 (DF6033), p-PERK (Thr-982), PERK (AF5304), p-eIF2 α (Ser-51/52) (AF3087), eIF2 α (AF6087), ATF4 (DF6008) were purchased from affinity biotech Cincinnati, OH, 45219, USA. Secondary antibody used goat anti-rabbit IgG HRP linked (HAF008), procured from R&D systems. For western blotting GAPDH (MAB374) antibody obtained by

Merckmillipore, Burlington, USA. We purchased Alexa Fluor 594 (mouse) from Invitrogen, Waltham, USA.

2.2. Animals

Complete protocols for the entire experiment were permitted by the Animal Ethics committee (IAEC/2018/F-26.), Council of Scientific and Industrial Research-Central Drug Research Institute (CSIR-CDRI, Lucknow, India). We received thirty healthy female (4–6 weeks old) Sprague Dawley (SD) rats from the National Animal Laboratory Centre of CSIR-CDRI. Rats were kept at optimum room temperature ($24 \pm 2^\circ\text{C}$) and relative humidity 50–60% with a regular 12-h light/dark cycle (lights on at 6 a.m. and lights off at 6 pm).

2.3. Experimental model development and study design

After one week of acclimatization, rats were divided into two groups, including the Control group and HVCD group. Olive oil (1 ml/kg) was injected as a vehicle in the Control group while VCD (80 mg/kg, 1 mL/kg of body weight) was injected intraperitoneally in the HVCD group for consecutive 17 days [24]. Control and HVCD group were fed with a standard chow diet during VCD treatment, while after completion of VCD and olive oil administration HVCD group was fed HFrD for 12 weeks.

2.4. Drug administration

Bodyweight alterations were measured during drug administration. In the 12th week, HVCD rats were randomly divided into 4 groups, including the HVCD group, HVCD + Met group, HVCD + PSTi8 group, HVCD + Comb group. We performed intraperitoneal glucose tolerance test (IPGTT) with Met (150 mg/kg) (Calixto et al., 2013; Salomäki et al., 2013), PSTi8 (5 mg/kg) [24] and Comb (Met 75 mg/kg + PSTi8 2.5 mg/kg) including 2 g/kg glucose load. We found glucose intolerance and IR concomitant to the cessation of the estrus cycle that manifests VCD induced ovarian follicle degradation. These findings confirmed the HFrD-induced dysregulation of lipid and glucose metabolism with reduced estrogen milieu mimicking perimenopausal conditions. Furthermore, Met (150 mg/kg) orally, PSTi8 (1 mg/kg) intraperitoneally and combination (Met 75 mg/kg + PSTi8 0.5 mg/kg) were administered for 14 days sequentially in rats, continued on HFrD. We performed IPGTT following the chronic treatment period to determine the impact of chronic medicament. Further, rats were euthanized by decapitation, and plasma samples were separated from the blood collected by retro-orbital puncture (centrifuged at 3000 g for 10 min). Collected tissues and plasma samples stored at -80°C until use.

2.5. Vaginal smears and estrus cycle determination

The estrous cycle stage was determined for ten consecutive days following 12 weeks of HFrD feeding and after completion of the treatment [25]. Cells were obtained by vaginal lavage on a slide and stained with the methylene blue stain. The extra stain was washed in running tap water and visualized under a light microscope. Animals were rated as anovulatory when they remained in the diestrus phase/metestrus phase indefinitely.

2.6. Measurement of body composition

Measurement of total lean mass and fat mass of rats were performed by EchoMRI body composition analyzer (E26-226-RM EchoMRI LLC, USA), according to the instructions provided [26].

2.7. Intraperitoneal glucose tolerance test

We performed IPGTT following 6 h fasting. Control and HVCD group rats were administered 0.9 % saline while HVCD + Met group was

administered with Met (150 mg/kg) (acute and chronic both), HVCD + PSTi8 group was administered with PSTi8 (5 mg/kg) (acute) or PSTi8 1 mg/kg (chronic) [24] and HVCD + Comb group was administered with Met 75 mg/kg + PSTi8 2.5 mg/kg (acute) or Met 75 mg/kg + PSTi8 0.5 mg/kg (chronic), before 30 min of glucose or insulin administration. Moreover, blood glucose was estimated at 0, 15, 30, 60, 90, 120 min after glucose (2 g/kg) administration. Graphpad prism software was used to calculate the area under curve (AUC).

2.8. Detection of serum estradiol level

For the detection of serum estradiol, mice fasted for 6 h, and blood was withdrawn from the ophthalmic vein. The level of estradiol was estimated in by ELISA Kit (ELK1208), following the instructions provided by the kit.

2.9. Plasma lipid profile detection

Plasma HDL-C levels were determined using High-density Lipoprotein Cholesterol (HDL-C) (E-BC-K221), plasma LDL-C detected by Low-density Lipoprotein Cholesterol (LDL-C) (E-BC-K205), and plasma triglycerides were detected by Colorimetric assay Kit (E-BC-K238). These kits were purchased from Elabscience Biotechnology Inc. Texas, USA.

2.10. Determination of liver function test markers

Markers of liver function tests, serum glutamic pyruvic transaminase (SGPT), serum glutamic oxaloacetic transaminase (SGOT), and alkaline phosphatase (ALP) were determined in collected serum using assay kits (Erba Mannheim).

2.11. Liver histopathology

For histopathological analysis of hepatic tissues, neutral buffered formalin was used to fix liver sections, followed by dehydration with 70, 90, and 100 % ethanol. After xylene treatment, tissue sections were rehydrated (with ethanol 100%, 70%, 50%) and stained (H & E stain). We analyzed captured images (20 X magnification (Leica DM-5000)) for the detection of hepatic steatosis and ballooning [27].

2.12. RNA isolation and qPCR

We utilized the TRIzol method to isolate total RNA from liver tissues. For RT-qPCR, cDNA was prepared by cDNA Reverse Transcription kit and SureCycler 8800 (Agilent Technologies, USA). We used LightCycler 480 Instrument II (Roche Life Science) for RT-qPCR. We used delta Ct values to determine relative mRNA expression. Sequences of primers used for this study enlisted in Table 1.

2.13. Immunoblotting

Liver tissue was homogenized in lysis buffer containing protease inhibitor cocktail and phosphatase inhibitor cocktail at 4 °C. Isolated protein from liver tissue lysates was used for western blotting. Primary antibodies used for immunoblotting are SIRT1, SREBP-1c, phospho-Insulin receptor substrate -1 (p-Ser307) (IRS-1), IRS-1, phospho-protein kinase B (p-Ser473) (p-AKT), Pan AKT, phospho-PERK (Thr-982), PERK, phospho-eIF2 α (Ser 51/52), eIF2 α , GRP78, ATF4 and GAPDH overnight at 4 °C. Protein bands obtained by myECL imager of Thermo Fischer Scientific Waltham, USA, were further normalized with their relevant controls and analyzed by Image J software (NIH, USA).

Table 1. List of primers.

<i>rSirt1</i>	F	TACCTTGAGAGCAGTTGCAG
	R	GCTTCATGATGGCAAGTGGC
<i>rSrebp1c</i>	F	ACAAGATTGTGGAGCTCAAGG
	R	TGCGCAAGACAGCAGATTTA
<i>rAcc1</i>	F	AGACCCAGTCTACATCCGCT
	R	TGCAAGTCAGCAAACCTGCAC
<i>rScd1</i>	F	GAAGCGAGCAACCCACAG
	R	GGTGGTCGTAGGAACCTGG
<i>rFas</i>	F	GGCCCATTTTGTCTCAA
	R	TCCACTTGTGTGCAGTCCT
<i>rCpt1a</i>	F	GTGAAGCCTTTGGGTGGATA
	R	TCTTTATGCAGGAACCCAGTAAGG
<i>rUcp2</i>	F	GACTCTGTAAGCAGTTCTACACCAA
	R	GGGCACCTGTGGTGTCTAC
<i>r18s</i>	F	CGCGGTTCTATTTTGTGGT
	R	AGTCGGCATCGTTTATGGTC

r: rat; F: forward; R: reverse.

2.14. Cell culture

HepG2 cell culture (ATCC, Manasses, VA, USA) was maintained in DMEM low glucose in the presence of 10 % FBS, antibiotics (L-Glutamine-Penicillin-Streptomycin solution), and humid atmosphere of 5 % CO₂ at 37 °C.

2.15. Nile Red and oil red O staining

Lipid accumulation in HepG2 cells was assessed by Nile Red and Oil Red O staining. Semi confluent cells were incubated with fructose (5 mM) [28, 29] with or without Met 100 μ M, PSTi8 200 nM, and combination (Met 50 μ M + PSTi8 100 nM) for 24 h. For Nile Red staining, the media was removed, washed with PBS twice, incubated with Nile Red stain, and analyzed by fluorescence microscope (Leica). For Oil Red O staining we followed the procedure described previously [27]. Furthermore, following drug treatment, cells were washed with phosphate buffered saline (PBS) (two times) then cultured cells were incubated with Oil Red O stain (0.36 % in 60 % isopropanol). The imaging for lipid droplets was examined in the bright field using the EVOS FL auto microscope (Life Science Technology) [30].

2.16. Immunofluorescence

We performed immunofluorescence analysis in HepG2 cells following the protocol established in our lab (Syed et al., 2020). Cells were maintained in low glucose media and incubated with fructose (5 mM) with or without Met 100 μ M, PSTi8 200 nM, and combination (Met 50 μ M + PSTi8 100 nM) for 24 h. Following the treatment, the media was removed and washed with PBS three times. Then, fixation and permeabilization of cells were done by cold methanol for 30 min. Excess methanol was removed and washed with PBS thrice. Blocking of cells was done by incubation of cells with 5% BSA for 2 h. Excess BSA was removed and washed with PBS, followed by incubation in primary antibody (anti-SIRT1, anti-SREBP-1c) overnight. The primary antibody was retrieved, washed 5 times with PBS, and treated with species-specific Alexa Fluor 594 for 2 h, the secondary antibody was removed, washed, and DAPI was added for nucleus staining. Imaging was done under a fluorescence microscope (Leica).

2.17. Statistical analysis

In the present study, results are displayed as means \pm SEM. GraphPad Prism software was used for data analysis. Statistical analysis was performed by using Student's t-tests and one or two-way ANOVA. Bonferroni

post-test was applied when required. Statistical significance was considered as $p < 0.05$.

3. Results

3.1. Experimental design and effect of combination therapy on VCD-induced perturbed estrous cycle of female rats

Experimental design and drug administration duration has been depicted in Figure 1a. VCD is an industrial chemical that promotes a selective loss of primordial follicles in the ovary. Persistent estrus or diestrus period for consistent 10 days or more represents an abnormal

estrus cycle [31]. The normal estrus cycle continues progressively and lasts for 4–5 days, as we found in the Control group (Figure 1b). We found an irregular estrus cycle in HVCD rats with persistent diestrus phase, while a combination of Met and PSTi8 brought down irregularities in the estrus cycle (Figure 1b). Figure 1c represents different phases of the estrus cycle. Additionally, we found reduced estrogen levels in the HVCD group; however, the combination of Met and PSTi8 restored estrogen levels at lower therapeutic doses than Met and PSTi8 alone, as indicated by the estrus cycle study (Figure 1d). These findings revealed that VCD treatment perturbed the normal estrus cycle while combination therapy restored it.

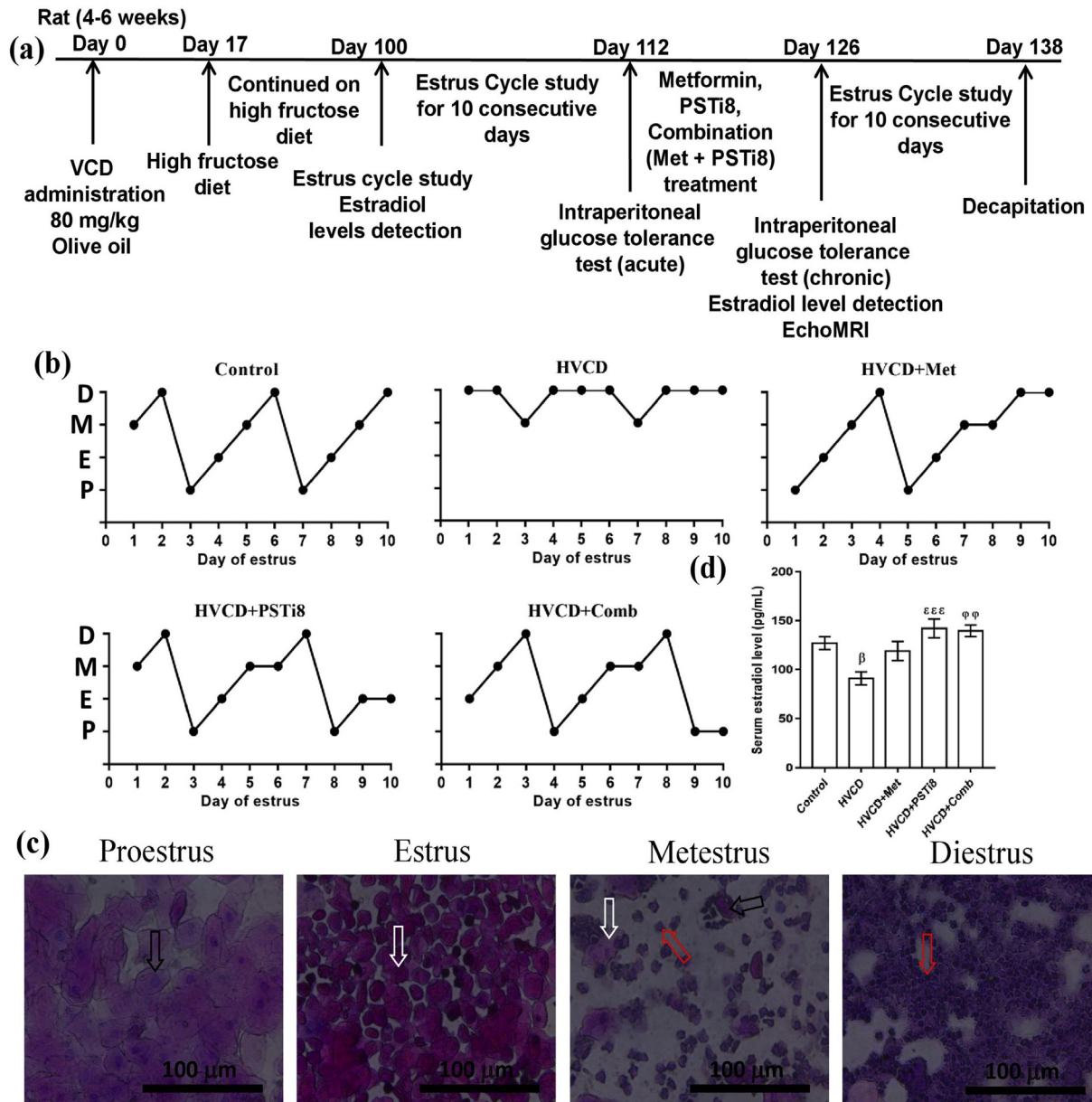


Figure 1. Estrus cycle study and examination of plasma estradiol level in HFrD/VCD-induced perimenopausal rat model. (a) Experimental design and treatment intervention (b) Estrus cycle evaluation for 10 days and stages of the estrus cycle, (c) representing different stages of estrus cycle including (d) serum estradiol level. P: proestrus phase characterized by the presence of nucleated epithelial cells (indicated by black arrow); E: estrus phase, characterized by the presence of cornified cells (indicated by white arrow); M: metestrus phase, characterized by the presence of nucleated epithelial cells, cornified cells, and leukocyte infiltration (indicated by the red arrow); D: diestrus, characterized by the presence of leukocyte infiltration. Results are shown as means \pm SEM ($n = 6$). Significance among different groups presented as β , Control vs HVCD, δ , HVCD vs HVCD + Met; ϵ , HVCD vs HVCD + PSTi8; ϕ , HVCD vs HVCD + Comb. Significance represented as β $p < 0.05$; ϕ $p < 0.01$; ϵ $p < 0.001$.

3.2. Effect of combination of Met and PSTi8 on body weight, fat mass, and glucose tolerance

We investigated body weight changes before and after drug administration to inspect how combination therapy administration at reduced doses affects body mass. We found enhanced bodyweight (Figure 2a) in HVCD rats, whereas combination treatment of Met and PSTi8 at reduced doses attenuated body weight. HVCD rats displayed increased fat mass percentage (Figure 2b), which might result from chronic high fructose consumption and enhanced lipogenesis. Met and PSTi8 alone doses significantly reduced fat mass, and similarly, combination therapy at reduced doses compared to alone Met and PSTi8 also reduced fat mass percent. Subsequently, the HVCD group displayed a significant loss of lean mass percent (Figure 2c). On the contrary, combination therapy recovered lean body mass percentage. Furthermore, we performed an intraperitoneal glucose tolerance test with 2 g/kg glucose challenge. HVCD rats showed glucose intolerance as we found that these rats were unable to counterbalance increased glucose load as they exhibited a sharp increase at initial 15 and 30 min, which showed defective insulin action in response to a glucose load. AUC analysis represented that combination therapy significantly ameliorated glucose intolerance during acute (Figure 2d–e) and more effectively with chronic (Figure 2f–g) drug administration. Combination treatment with decreased therapeutic doses of Met and PSTi8 inhibited blood glucose increase at an initial 15 and 30 min. It maintained basal blood glucose at 120 min, which revealed that a combination of Met and PSTi8 restored insulin action.

3.3. Met and PSTi8 combination therapy improved liver function

Liver function markers such as SGPT, SGOT, and ALP are previously evidenced to be increased in obesity, dyslipidemia, and diabetes [32]. Parallely, we found an enhanced level of these enzymes in the HVCD group (Figure 3). Combination therapy of Met and PSTi8 at lower doses

in comparison to full Met and PSTi8 alone doses ameliorated serum level of SGPT, SGOT, and ALP enzymes (Figure 3).

3.4. Met and PSTi8 combination improved plasma lipid profile, inhibited hepatic lipid accumulation in HVCD-induced perimenopausal rats

In accordance with previous studies, it has been suggested that an HFrD enhances ectopic lipid accumulation by increasing lipid load [33]. Therefore, we investigated the plasma lipid profile and hepatic lipid accumulation in HVCD rats. We found a notable increase in LDL (Figure 4a), VLDL (Figure 4c), TG (Figure 4d), and TC (Figure 4e) plasma levels and a decrease in HDL (Figure 4b) level in the HVCD group. Combination therapy at lower therapeutic doses in comparison to alone Met and PSTi8 significantly decreased plasma LDL, VLDL, TG, and TC levels. The present combination also restored HDL levels in the plasma of HFrD perimenopausal rats. Additionally, HFrD-induced adverse effects on hepatic lipid accumulation were detected by H & E staining of liver sections (Figure 4f). We detected steatosis (Figure 4g) and increased ballooning score (Figure 4h) in the liver of HVCD perimenopausal rats. Intriguingly, Met and PSTi8 in combination attenuated steatosis and ballooning in the perimenopausal rats.

3.5. Met and PSTi8 combination attenuated lipid accumulation in HFr-induced insulin-resistant HepG2 cells

To further demonstrate the notion that high fructose (HFr) exposure may cause ectopic lipid accumulation, we detected lipid accumulation in HepG2 cells in the presence of HFr. Nile Red staining (Figure 5a, c) and Oil Red O staining (Figure 5b, d) displayed higher lipid accumulation in HFr-induced HepG2 cells. Combination therapy of Met and PSTi8 at lower doses in comparison to alone Met and PSTi8 attenuated lipid accumulation in insulin-resistant HepG2 cells.

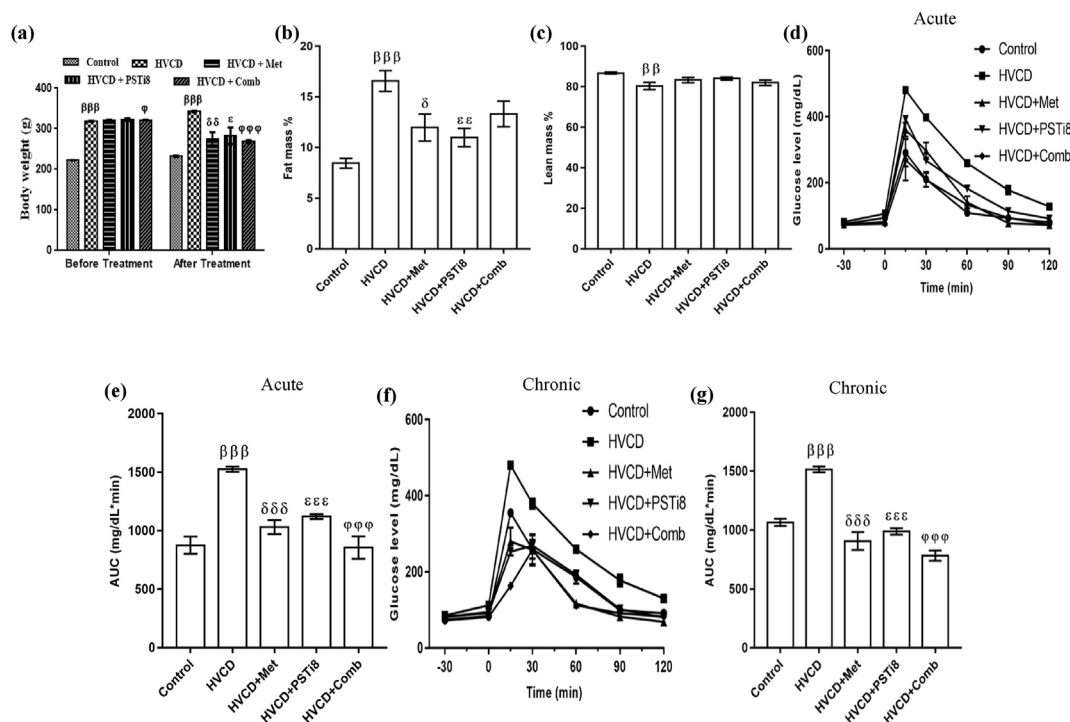


Figure 2. HFrD fed perimenopausal rat model development and effect of combination therapy on glucose intolerance. (a) body weight, (b) complete fat mass %, (c) complete lean mass %, (d) IPGTT and its relevant (e) AUC with acute treatment of Met 150 mg/kg, PSTi8 5 mg/kg and combination Met 75 mg/kg + PSTi8 2.5 mg/kg, including glucose 2 g/kg, (f) IPGTT and its relevant (g) AUC with chronic treatment of Met 150 mg/kg, PSTi8 1 mg/kg, and combination Met 150 mg/kg + PSTi8 0.5 mg/kg and glucose 2 g/kg. Results are shown as means ± SEM (n = 6). Significance among different groups presented as β, Control vs HVCD; δ, HVCD vs HVCD + Met; ε, HVCD vs HVCD + PSTi8; φ, HVCD vs HVCD + Comb. Significance demonstrated as δp<0.05; ββp<0.01; βββ,δδδ,εεε,φφφφp<0.001.

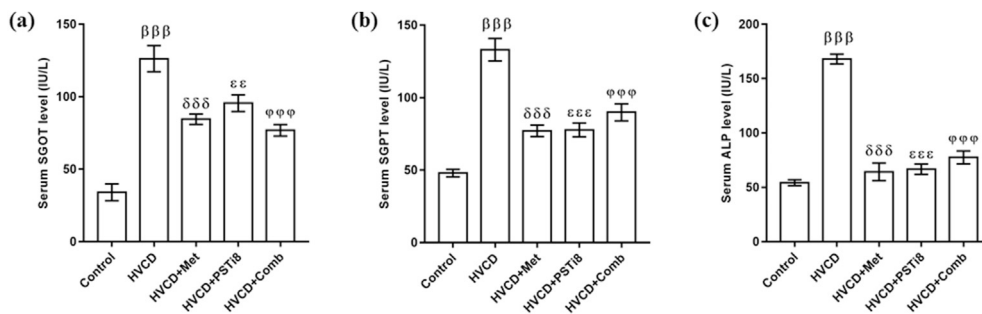


Figure 3. Effect of combination therapy on important elements of liver function. (a) SGOT, (b) SGPT, and (c) serum ALP. Comparative significance results are shown as means \pm SEM (n = 6). Significance among groups presented as β , Control vs HVCD, δ , HVCD vs HVCD + Met; ϵ , HVCD vs HVCD + PSTi8; ϕ , HVCD vs HVCD + Comb. Significance presentation as $\epsilon\epsilon$ $p < 0.01$; $\beta\beta\beta, \delta\delta\delta, \epsilon\epsilon\epsilon, \phi\phi\phi$ $p < 0.001$.

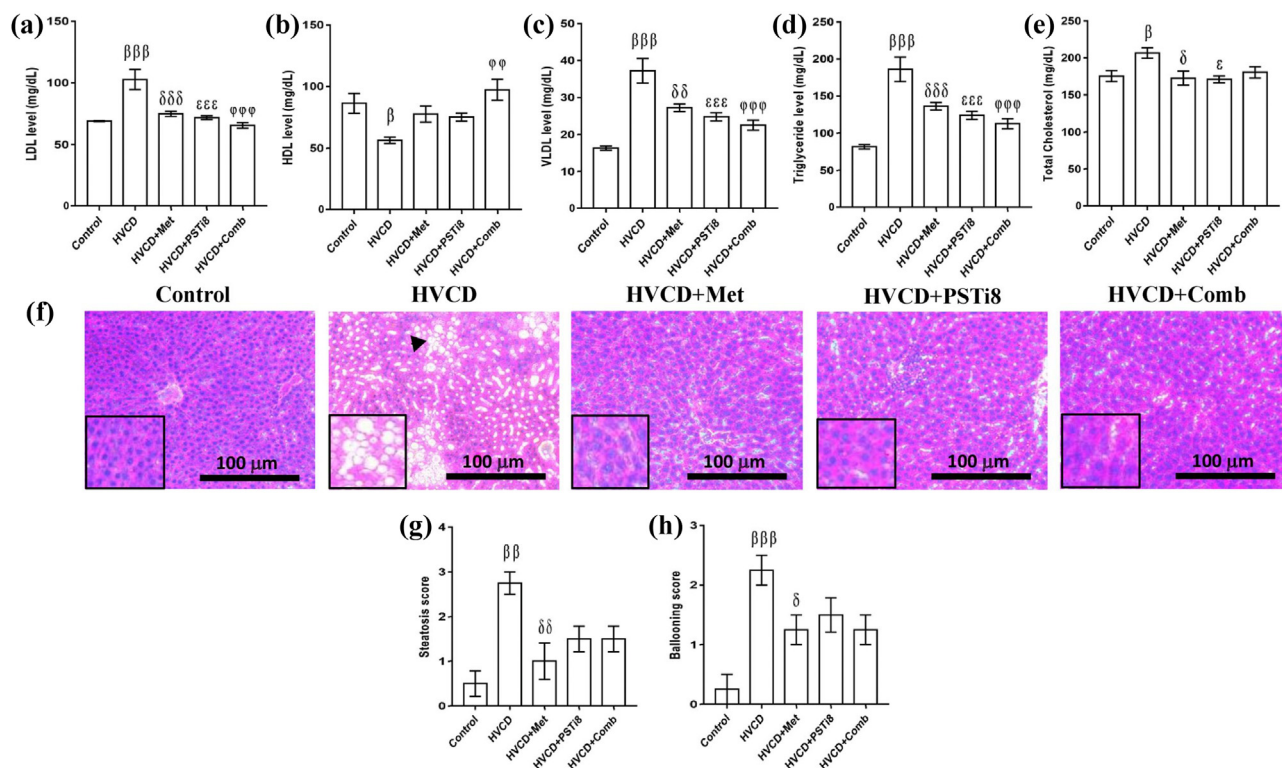


Figure 4. Combination therapy ameliorated plasma lipid markers and reduced hepatic lipid deposition. Plasma lipid markers (a) LDL, (b) HDL, (c) VLDL, (d) triglyceride, and (e) total cholesterol. (f) Liver histopathological analysis was performed by staining with H & E stain (scale bar 100 μ m, 20x magnification). (g) Liver steatosis score analysis and (h) hepatic ballooning score analysis. Data represented as means \pm SEM (n = 6). Significance among different groups presented as β , Control vs HVCD, δ , HVCD vs HVCD + Met; ϵ , HVCD vs HVCD + PSTi8; ϕ , HVCD vs HVCD + Comb. Significance illustrated as β, δ, ϵ $p < 0.05$; $\beta\beta, \delta\delta, \epsilon\epsilon, \phi\phi$ $p < 0.01$; $\beta\beta\beta, \delta\delta\delta, \epsilon\epsilon\epsilon, \phi\phi\phi$ $p < 0.001$.

3.6. Met and PSTi8 in combination attenuated hepatic lipotoxicity by activating SIRT1 in high fructose exposed HepG2 cells and in the liver of HFrD/VCD-induced perimenopausal rats

It has been speculated that SIRT1 overexpression mitigates ER stress and steatosis [34]. Therefore, we investigated the expression of SIRT1 in the presence of HFr load. We found reduced fluorescence intensity of SIRT1 in HFr exposed HepG2 cells (Figure 6a,b). Contrary to this, combination therapy of Met and PSTi8 at half of the alone therapeutic doses increased the intensity of SIRT1 fluorescence in the presence of HFr load (Figure 6a, b). In line with these findings, combination treatment of Met and PSTi8 also increased mRNA (Figure 6c) and protein expression (Figure 6d) of SIRT1 in HVCD-induced perimenopausal rats, which was inhibited by HFrD and in the presence of reduced estrogen milieu.

3.7. Combination therapy of Met and PSTi8 ameliorates hepatic lipid metabolism by inhibiting SREBP-1c in HFr-induced HepG2 cells and HVCD-instigated perimenopausal rats

The liver is the master organ involved in lipid synthesis amenable to TG synthesis. SREBP-1c is the key element of lipid synthesis, sensitive to nutritional status [35]. We detected increased fluorescence intensity of SREBP-1c in HFr-induced HepG2 cells (Figure 7a,b). On the other hand, a combination of Met and PSTi8 at the half of individual Met and PSTi8 therapeutic doses significantly reduced the fluorescence intensity of SREBP-1c in the presence of HFr exposure (Figure 7a,b). Likewise, we detected enhanced hepatic mRNA (Figure 7c) and protein expression (Figure 7d) of SREBP-1c in the HVCD group. At the same time, a combination of Met and PSTi8 significantly attenuated SREBP-1c expression as equivalent to Met and PSTi8 monotherapy.

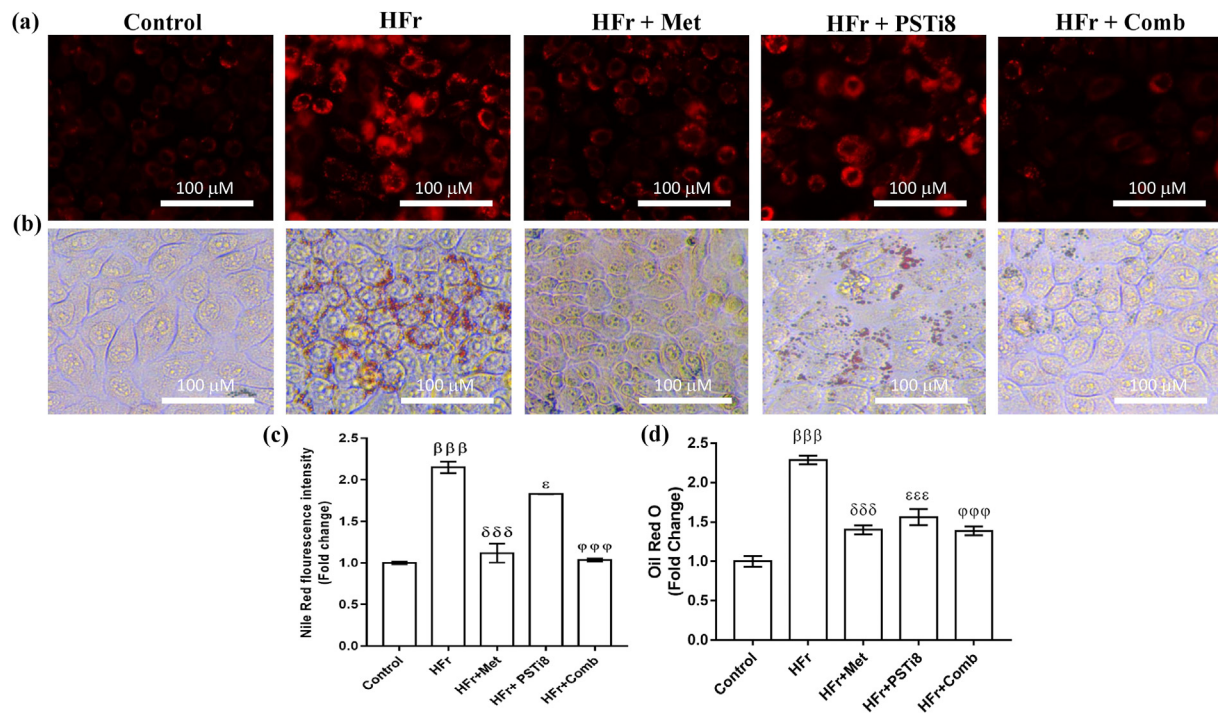


Figure 5. Combination therapy attenuated lipid accumulation in high fructose-induced insulin-resistant HepG2 cells. (a) Nile Red staining to detect lipid accumulation in HFr-induced HepG2 cells and (b) Oil Red O staining (c) Nile Red fluorescence intensity quantification. (d) Quantification of lipid accumulation detected by Oil Red O staining in HFr-induced HepG2 cells. Results were represented as means \pm SEM ($n = 6$). Significance among different groups presented as β , Control vs HFr; δ , HFr vs HFr + Met; ϵ , HFr vs HFr + PSTi8; ϕ , HFr vs HFr + Comb. Significance represented as * $p < 0.05$; $\beta\beta\beta, \delta\delta\delta, \epsilon\epsilon\epsilon, \phi\phi\phi p < 0.001$.

Furthermore, we investigated downstream regulators of SREBP-1c involved in *de-novo* lipid synthesis as FAS, ACC1, SCD1 (Figure 7 e–g). We found increased mRNA expression of FAS, ACC1, and SCD1 in the HVCD group. At the same time, the combination Met and PSTi8 at lower doses significantly reduced lipogenesis by downregulating the expression of the aforementioned markers (Figure 7 e–g). Additionally, we observed enhanced expression of fatty acid oxidation associated genes, including Carnitine palmitoyltransferase-1 α (CPT1 α) (Figure 7 h) and uncoupling protein 2 (UCP2) (Figure 7 i) by combination therapy. In contrast, in the HVCD group, due to increased expression of SREBP-1c, fat oxidation was inhibited as manifested by reduced expression of CPT1 and UCP2.

3.8. Combination therapy of Met and PSTi8 alleviated ER stress-induced UPR and improved hepatic insulin sensitivity

It has been previously evidenced that a plethora of lipid supply may cause perturbations in protein folding homeostasis [36]. Thereby, we investigated ER stress UPR in the liver of HVCD perimenopausal rats. The HVCD group displayed increased expression of the PERK-eIF2 α -ATF4 axis, which results in the increased expression of GRP78 protein expression (Figure 8a), concomitant to the phosphorylation of PERK (Figure 8b) and eIF2 α (Figure 8c) proteins and also enhanced expression of ATF4 (Figure 8d). Simultaneously, compared to individual Met and PSTi8, combining a reduced dose of Met and PSTi8 downregulated GRP78, along with reduced phosphorylation of PERK, eIF2 α and expression of ATF4 proteins. This reduced ER stress by the combination of Met and PSTi8 preserved hepatic insulin signaling by inhibiting p-IRS (ser-307) (Figure 8e) and activating p-AKT (ser-473) (Figure 8f). At the same time, HFrD with VCD treatment disrupted insulin signaling by activating inhibitory phosphorylation of IRS1 and preventing activation of AKT. Altogether, these findings uncovered that the combination of Met and PSTi8 at reduced therapeutic doses

effectively ameliorates hepatic steatosis-induced ER stress and uphold hepatic insulin signaling.

4. Discussion

ER is identified as a protein folding cellular machinery engaged in synthesis, folding, assembly, and modification of soluble and membrane proteins [37]. This vivacious system of protein folding adapts protein folding capacity according to the physiological requirements of the cells [38]. When physiological states or cellular demand for protein folding exceeds ER capacity, that results in a conglomeration of misfolded and unfolded proteins, further proceeds into UPR. ER in hepatocytes have the exquisite capacity to adapt to extracellular and intracellular stimuli. However, obesity and hepatic steatosis may perturb hepatic lipid metabolism culminating into ER stress [39, 40].

Previously Met and PSTi8 combined efficiently improved hepatic metabolism and reversed hepatic lipid accumulation [23]. The present study results point towards the potential role of the combination of Met and PSTi8 at reduced therapeutic doses in ameliorating hepatic steatosis linked to ER stress and IR in perimenopausal rats. VCD-induced follicular atresia leads to the natural progression of menopause, renders females more prone to develop hepatic steatosis [41, 42, 43]. Accordingly, with these findings, we studied estrus phases in VCD treated rats for 10 consecutive days following 12 weeks of HFrD feeding. We found that HVCD displayed a consistent diestrus phase (Figure 1b), hence an irregular estrus cycle. This loss of ovarian follicle was also confirmed by reduced estrogen release as observed in the HVCD group (Figure 1b). A combination of Met and PSTi8 at reduced therapeutic doses preserved the estrus cycle in HVCD rats by maintaining cyclicity comprising proestrus, estrus, metestrus, and diestrus phases (Figure 1b). The combination treatment reversed this estrogen loss might be by protecting primordial ovarian follicles. Furthermore, increased body weight has been discerned in VCD-induced rodents [43]. Likewise, the HVCD group exhibited enhanced bodyweight (Figure 2a) and increased fat mass

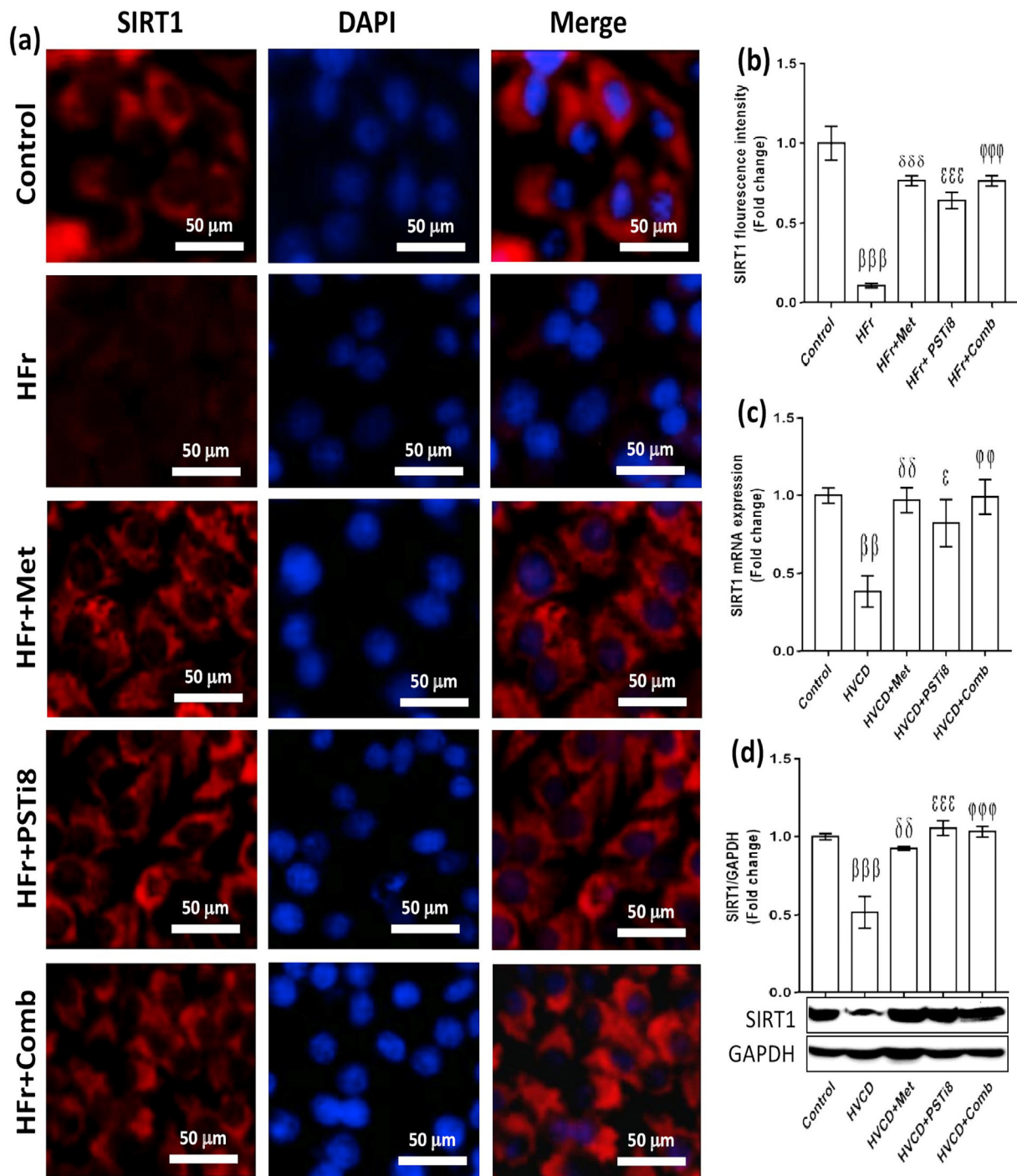


Figure 6. Combination therapy activates SIRT1 in HepG2 cells and liver of perimenopausal rats. (a) Immunofluorescence imaging of SIRT1 in HFr-induced HepG2 cells, (b) SIRT1 fluorescence intensity quantification (n = 6). (c) SIRT1 relative mRNA expression (n = 6) and (d) protein content (n = 3) in the liver of HVCD rats. SIRT1 mRNA and protein expression normalized with 18s and GAPDH expression, respectively (densitometry by Image J software). Results were represented as means ± SEM (n = 3). For (a and b), Significance among different groups presented as β, Control vs HFr; δ, HFr vs HFr + Met; ε, HFr vs HFr + PSTi8; φ, HFr vs HFr + Comb. For (c and d), significance values represented as β, Control vs HVCD; δ, HVCD vs HVCD + Met; ε, HVCD vs HVCD + PSTi8; φ, HVCD vs HVCD + Comb. Significance showed as ^εp<0.05; ^{δδ}p<0.01; ^{βββ,δδδ,εεε, φφφ}p<0.001.

percentage (Figure 2b) while reduced lean mass percentage (Figure 2c). A combination of Met and PSTi8 at lower doses, compared to full doses of Met and PSTi8 manifested propitious effects by maintaining body weight and total body fat mass percentage (Figure 2a–c).

Intriguingly, VCD-induced perimenopausal rats have been demonstrated to develop glucose intolerance [24, 41]. Similarly, we also noticed attenuated glucose intolerance in the HVCD group. At the same

time, combinatorial therapy of Met and PSTi8 at reduced doses compared to alone higher therapeutic doses improved glucose tolerance during acute (Figure 2d, e) and more effectively during chronic treatment regimen (Figure 2f, g). One apparent description would be that HFr consumption combined with VCD treatment undermined hepatic lipid homeostasis, consequently disrupting insulin response towards glucose load resulting in glucose intolerance. Contrarily, results indicated that

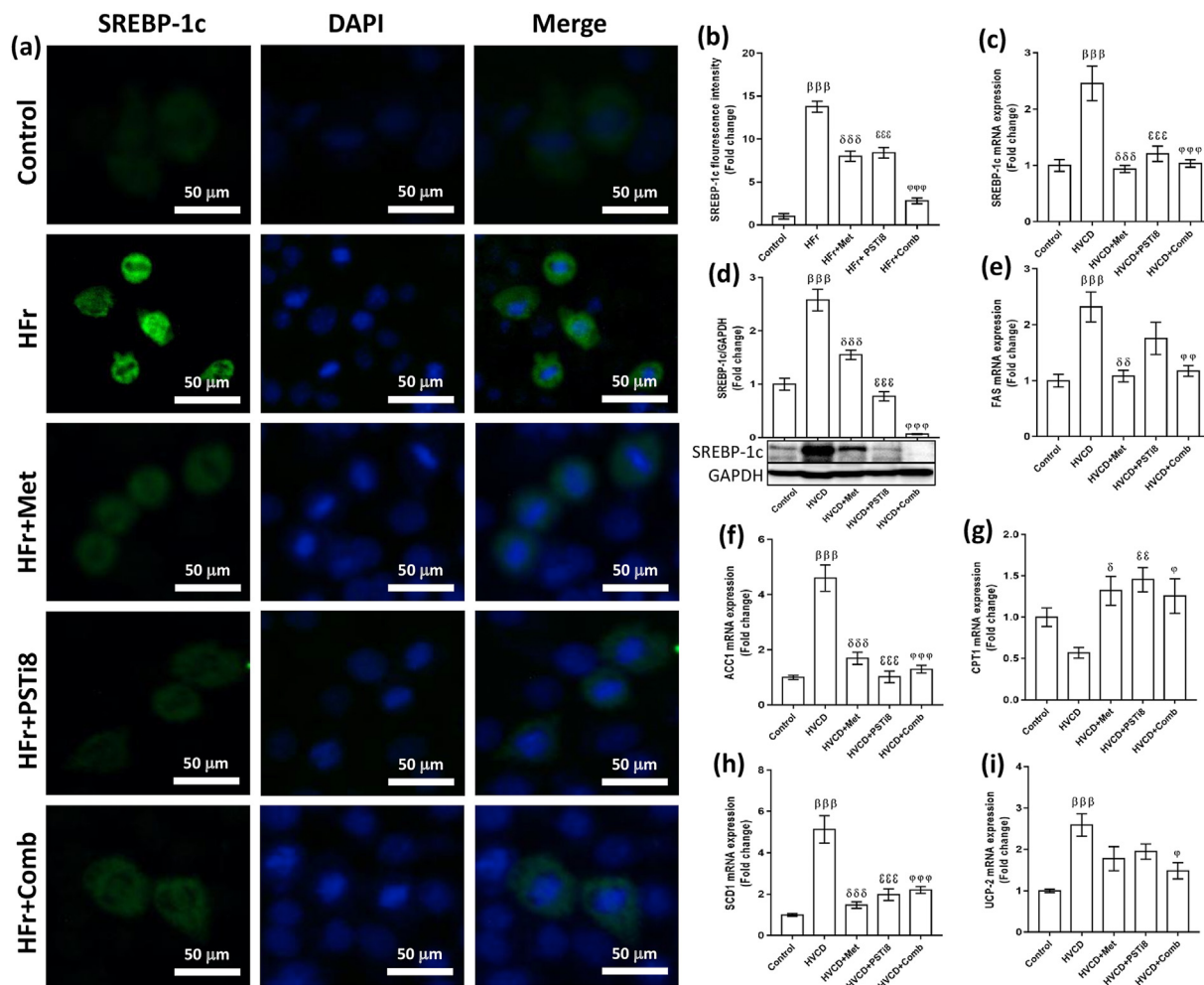


Figure 7. Combination therapy improved SREBP-1c expression in HFr induced HepG2 cells and hepatic SREBP-1c expression in perimenopausal rats. (a) Immunofluorescence imaging of HFr-induced HepG2 cells, (b) SREBP-1c fluorescence intensity quantification (n = 6). (c) Relative mRNA expression of SREBP-1c in the liver, studied by qRT-PCR (n = 6). (d) Total form of SREBP-1c (molecular weight 122kDa) presented by western blotting indicates protein expression levels (n = 3). We investigated relative mRNA expression of downstream markers of SREBP-1c. These are represented as (e) FAS (f) ACC-1 (g) SCD-1. Further, we determined the relative mRNA expression of fat oxidation related genes (h) CPT-1a (i) UCP-2. The mRNA and protein expressions were normalized with corresponding 18s and GAPDH expression, respectively. Results were represented as means ± SEM (n = 6). For (a and b), significance among different groups displayed as β, Control vs HFr; δ, HFr vs HFr + Met; ε, HFr vs HFr + PSTi8; φ, HFr vs HFr + Comb. For (c to i), Significance among groups showed as β, Control vs HVCD; δ, HVCD vs HVCD + Met; ε, HVCD vs HVCD + PSTi8; φ, HVCD vs HVCD + Comb. Significance represented as ^φp<0.05, ^{δδ}p<0.01, ^{βββ,δδδ,εεε,φφφφ}p<0.001.

Met and PSTi8, in combination, efficaciously improved tolerance to glucose.

Previous studies persuaded that liver-specific enzymes such as SGPT, SGOT, and ALP are intensely sensitive markers for liver damage and were found to be increased during hepatic injury [44]. This could be correlated with increased SGOT, SGPT, and ALP serum levels in the HVCD group (Figure 3a–c). Significant reduction in serum level of these markers by combination therapy explains that Met and PSTi8 in combination at reduced doses are hepatoprotective and effective in preventing liver injury.

It was convincingly demonstrated that HFrD (60% fructose) elevated key lipid parameters in plasma, including plasma TG and LDL concentrations [45, 46]. In agreement with these reports, we also found increased plasma TG, LDL, VLDL, and TC levels while reduced plasma HDL levels in the HVCD group (Figure 4a–e). Alleviated plasma TG, LDL, VLDL, and total cholesterol levels and enhanced plasma HDL in HFrD fed perimenopausal rats by combination therapy demonstrated that Met and PSTi8 in combination are possibly working towards the regulation of plasma lipid levels and maintaining lipid homeostasis. Consequently, this raised the possibility that Met and PSTi8 in combination may inhibit ectopic lipid accumulation in the liver. Therefore, we studied hepatic

lipid accumulation by H & E staining (Figure 4f) and found that combination therapy attenuated lipid droplet formation in the liver manifested reduced steatotic score (Figure 4g) and minimized hepatic ballooning score (Figure 4h). To further validate these interesting findings, we investigated lipid accumulation in HFr-induced HepG2 cells. Moreover, combination therapy reduced oil droplet formation in HFr-induced HepG2 cells, as evidenced by reduced fluorescence intensity detected by Nile Red staining (Figure 5a and c). In addition, Oil Red O staining results also demonstrated that a combination of Met and PSTi8 could effectively reduce HFr-induced lipid accumulation (Figure 5b and d). Furthermore, it has been demonstrated that hepatic steatosis is closely associated with the emergence of ER stress [47]. Moreover, SIRT1 has been demonstrated to attenuate hepatic steatosis and, consequently, hepatic ER stress and IR [34]. Further studies suggested that SIRT1 overexpression prevents lipid accumulation in steatotic hepatocytes [48]. Hence, we were puzzled that if SIRT1 activation and attenuated *denovo* lipogenesis are effective in ameliorating ER stress and IR in HFrD fed perimenopausal rats. Herein, results displayed combination therapy increased fluorescence intensity of SIRT1 in HFr induced HepG2 cells and enhanced mRNA and protein expression of SIRT1 in HFrD fed perimenopausal rats. These outcomes strengthened the possibility that

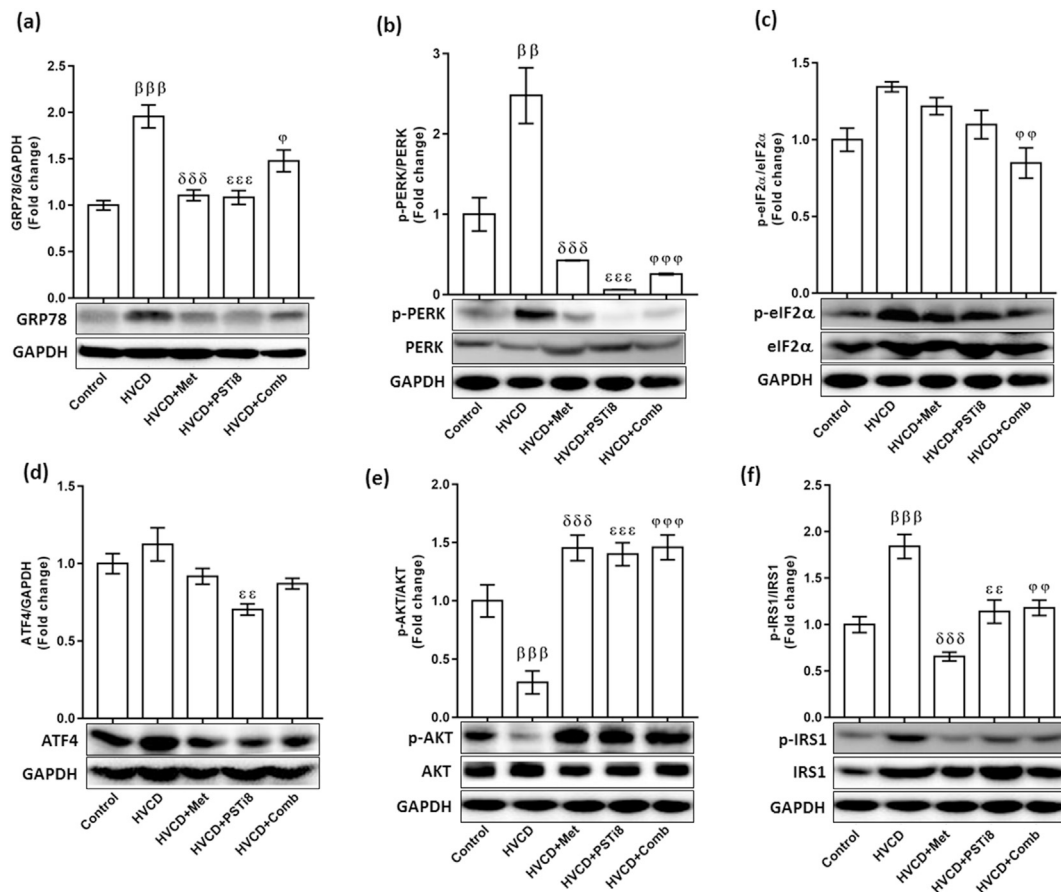


Figure 8. Combination therapy ameliorated the ER stress-induced PERK-eIF2 α pathway and improved insulin signaling. We detected protein expression levels of hepatic ER stress pathway (a) GRP78, (b) p-PERK, and (c) p-eIF2 α (d) ATF4. Concomitantly combination of Met and PSTi8 improved insulin sensitivity in liver as identified by improved insulin signaling. We detected protein phosphorylation of (e) p-(Ser-473) AKT (f) p-(Ser-307) IRS-1. Results are presented as means \pm SEM ($n = 3$). Significance among groups presented as β , Control vs HVCD; δ , HVCD vs HVCD + Met; ϵ , HVCD vs HVCD + PSTi8; ϕ , HVCD vs HVCD + Comb. Significance represented as $^{\phi}p < 0.05$; $^{\beta\beta\beta\epsilon\epsilon\phi\phi}p < 0.01$; $^{\beta\beta\beta,\delta\delta\delta,\epsilon\epsilon\epsilon,\phi\phi\phi}p < 0.001$.

combination therapy may effectively reduce de novo lipogenesis by activation of SIRT1. Moreover, SREBP-1c has been shown to be activated by fructose in mice [49]. High fructose feeding stimulates the expression of SREBP-1c and additional lipogenesis related genes (ACC, FAS, SCD1) [50]. Concomitantly, we found that a combination of Met and PSTi8 attenuated SREBP-1c fluorescence intensity in HFr induced insulin-resistant HepG2 cells, and also mRNA and protein expression of SREBP-1c in HFrD fed perimenopausal rats (Figure 6). Likewise, combination treatment decreased the expression of downstream signaling markers of SREBP-1c: FAS, ACC, SCD-1 (Figure 7) and eventually attenuated hepatic lipogenesis. Conversely, we found enhanced hepatic expression of CPT1a (Figure 7h) and UCP2 (Figure 7i) mRNA levels, apparently displayed enhanced fatty acid oxidation in the liver. One reasonable explanation might be that HFrD fed perimenopausal rats have lost their ability to oxidize excess lipids contributed by HFrD and reduced estrogen milieu. Simultaneously, Met and PSTi8, in combination, reversed these anomalies by enhancing fat oxidation, attenuating ectopic lipid accumulation, and, consequently, ER stress.

There are three peculiar ER transmembrane sensors, which lead to the activation of UPR: inositol-requiring 1 α (IRE1 α), PERK, and ATF6 [51]. Of note, uncurbed hepatic lipogenesis induced steatosis by HFr feeding exacerbates activated PERK-UPR branch [52, 53]. It is well reported that hepatic ER stress and adaptive UPR pathways are elegantly associated with lipotoxicity [54]. PSTi8 has previously been explained that it interacts with GRP78 and inhibits PST action [20]. Additionally, Met has been mentioned to inhibit GRP78 chaperon protein [55]. In addition to this, ATF4 deficient mice exhibited protection against steatosis

development [56]. Conclusively, with these compelling findings, combination treatment of Met and PSTi8 at reduced therapeutic doses meticulously revealed diminished hepatic ER stress by mitigating the PERK-eIF2 α -ATF4 arm of UPR (Figure 8a–d). Moreover, combination therapy of Met and PSTi8 improved hepatic insulin signaling by regulating key elements of insulin signaling. Consequently, Met and PSTi8 in combination at lower doses escalated p-AKT (Ser-473) (Figure 8e) and reduced the expression of p-IRS (Ser-307) (Figure 8f). These results undoubtedly represented that combination of Met and PSTi8 may effectively reverse hepatic steatosis induced ER stress and improve insulin signaling.

5. Conclusion

Altogether, our results provide persuasive evidence that Met and PSTi8 in combination may potentially reverse hepatic steatosis associated ER stress and pertinent IR in HFrD fed perimenopausal rats by governing SIRT1/SREBP-1c axis. Hence, the present study may provide remarkable avenues towards therapeutic interventions and presumably fill gaps towards insights into the development of steatosis, ER stress, and IR.

Declarations

Author contribution statement

J.R. Gayen: Conceived and designed the experiments; Contributed reagents, materials, analysis tools or data; Wrote the paper.

P. Singh: Conceived and designed the experiments; Performed the experiments; Analyzed and interpreted the data; Wrote the paper.

M.I. Reza, A.A. Syed, R. Garg, A. Husain, R. Katekar, U.K. Goand, M. Riyazuddin and A.P. Gupta: Performed the experiments; Analyzed and interpreted the data.

Funding statement

J.R. Gayen was supported by CSIR, Govt. of India; DST, Govt. of India, and DBT, Govt. of India. CDRI communication number for this article is 10168.

Data availability statement

Data included in article/supplementary material/referenced in article.

Declaration of interests statement

The authors declare no conflict of interest.

Additional information

No additional information is available for this paper.

References

- H. Jo, S.S. Choe, K.C. Shin, H. Jang, J.H. Lee, J.K. Seong, S.H. Back, J.B. Kim, Endoplasmic reticulum stress induces hepatic steatosis via increased expression of the hepatic very low-density lipoprotein receptor, *Hepatology* 57 (2013) 1366–1377.
- C. Hetz, K. Zhang, R.J. Kaufman, Mechanisms, regulation and functions of the unfolded protein response, *Nat. Rev. Mol. Cell Biol.* 21 (2020) 421–438.
- X. Liu, R.M. Green, Endoplasmic reticulum stress and liver diseases, *Liver Res.* 3 (2019) 55–64.
- J. Tian, Q. Wu, Y. He, Q. Shen, M. Rekep, G. Zhang, J. Luo, Q. Xue, Y. Liu, Zonisamide, an antiepileptic drug, alleviates diabetic cardiomyopathy by inhibiting endoplasmic reticulum stress, *Acta Pharmacol. Sin.* (2020) 1–11.
- A.H. Lee, E.F. Scapa, D.E. Cohen, L.H. Glimcher, Regulation of hepatic lipogenesis by the transcription factor XBP1, *Science* 320 (2008) 1492–1496.
- K. Yamamoto, K. Takahara, S. Oyadomari, T. Okada, T. Sato, A. Harada, K. Mori, Induction of liver steatosis and lipid droplet formation in ATF6 α -knockout mice burdened with pharmacological endoplasmic reticulum stress, *Mol. Biol. Cell* 21 (2010) 2975–2986.
- S. Oyadomari, H.P. Harding, Y. Zhang, M. Oyadomari, D. Ron, Dephosphorylation of translation initiation factor 2 α enhances glucose tolerance and attenuates hepatosteatosis in mice, *Cell Metabol.* 7 (2008) 520–532.
- J.N. Lee, J. Ye, Proteolytic activation of sterol regulatory element-binding protein induced by cellular stress through depletion of Insig-1, *J. Biol. Chem.* 279 (2004) 45257–45265.
- U. Ozcan, Q. Cao, E. Yilmaz, A.-H. Lee, N.N. Iwakoshi, E. Özdelen, G. Tuncman, C. Görgün, L.H. Glimcher, G.S. Hotamisligil, Endoplasmic reticulum stress links obesity, insulin action, and type 2 diabetes, *Science* (80-.) 306 (2004) 457–461.
- J.C. Cohen, J.D. Horton, H.H. Hobbs, Human fatty liver disease: old questions and new insights, *Science* 332 (2011) 1519–1523.
- C. Lebeaupin, D. Vallée, Y. Hazari, C. Hetz, E. Chevet, B. Bailly Maitre, Endoplasmic reticulum stress signalling and the pathogenesis of non-alcoholic fatty liver disease, *J. Hepatol.* 69 (2018) 927–947.
- J.T. Rodgers, C. Lerin, Z. Gerhart-Hines, P. Puigserver, Metabolic adaptations through the PGC-1 α and SIRT1 pathways, *FEBS Lett.* 582 (2008) 46–53.
- H. Yamamoto, K. Schoonjans, J. Auwerx, Sirtuin functions in health and disease, *Mol. Endocrinol.* 21 (2007) 1745–1755.
- Q. Chen, X. Yang, H. Zhang, X. Kong, L. Yao, X. Cui, Y. Zou, F. Fang, J. Yang, Y. Chang, Metformin impairs systemic bile acid homeostasis through regulating SIRT1 protein levels, *Biochim. Biophys. Acta (BBA)-Mol. Cell Res.* 1864 (2017) 101–112.
- A. Prola, J.P. Da Silva, A. Guilbert, L. Lecru, J. Piquereau, M. Ribeiro, P. Mateo, M. Gressette, D. Fortin, C. Boursier, SIRT1 protects the heart from ER stress-induced cell death through eIF2 α deacetylation, *Cell Death Differ.* 24 (2017) 343–356.
- B. Ponugoti, D.H. Kim, Z. Xiao, Z. Smith, J. Miao, M. Zang, S.Y. Wu, C.M. Chiang, T.D. Veenstra, J.K. Kemper, SIRT1 deacetylates and inhibits SREBP-1C activity in regulation of hepatic lipid metabolism, *J. Biol. Chem.* 285 (2010) 33959–33970.
- E. Cuyàs, S. Verdura, L. Llorach Parés, S. Fernández Arroyo, J. Joven, B. Martín-Castillo, J. Bosch-Barrera, J. Brunet, A. Nonell-Canals, M. Sanchez-Martinez, Metformin is a direct SIRT1-activating compound: computational modeling and experimental validation, *Front. Endocrinol. (Lausanne).* 9 (2018) 657.
- W. Wang, X.H. Guo, H.H. Wu, N.H. Wang, X.S. Xu, Effect of fenofibrate and metformin on lipotoxicity in OLETF rat kidney, *Beijing Da Xue Xue Bao. Yi Xue Ban, J. Peking Univ. Heal. Sci.* 38 (2006) 170.
- J. Jin, Y. Ma, X. Tong, W. Yang, Y. Dai, Y. Pan, P. Ren, L. Liu, H.Y. Fan, Y. Zhang, Metformin inhibits testosterone-induced endoplasmic reticulum stress in ovarian granulosa cells via inactivation of p38 MAPK, *Hum. Reprod.* 35 (2020) 1145–1158.
- Z. Hossain, G.R. Valicherla, A.P. Gupta, A.A. Syed, M. Riyazuddin, S. Chandra, M.I. Siddiqi, J.R. Gayen, Discovery of pancreastatin inhibitor PSTi8 for the treatment of insulin resistance and diabetes: studies in rodent models of diabetes mellitus, *Sci. Rep.* 8 (2018) 1–13.
- A.P. Gupta, R. Garg, P. Singh, U.K. Goand, A.A. Syed, G.R. Valicherla, M. Riyazuddin, M.N. Mugale, J.R. Gayen, Pancreastatin inhibitor PSTi8 protects the obesity associated skeletal muscle insulin resistance in diet induced streptozotocin-treated diabetic mice, *Eur. J. Pharmacol.* (2020) 173204.
- U.S. Pettersson, T.B. Waldén, P.-O. Carlsson, L. Jansson, M. Phillipson, Female mice are protected against high-fat diet induced metabolic syndrome and increase the regulatory T cell population in adipose tissue, *PLoS One* 7 (2012) 46057.
- P. Singh, R. Garg, U.K. Goand, M. Riyazuddin, M.I. Reza, A.A. Syed, A.P. Gupta, A. Husain, J.R. Gayen, Combination of Pancreastatin inhibitor PSTi8 with metformin inhibits Fetuin-A in type 2 diabetic mice, *Heliyon* 6 (2020), 05133.
- G.R. Valicherla, A.P. Gupta, Z. Hossain, M. Riyazuddin, A.A. Syed, A. Husain, S. Lahiri, K.M. Dave, J.R. Gayen, Pancreastatin inhibitor, PSTi8 ameliorates metabolic health by modulating AKT/GSK-3 β and PKC α /SREBP1c pathways in high fat diet induced insulin resistance in peri-/post-menopausal rats, *Peptides* 120 (2019) 170147.
- S.M.M. Omar, E.L.S.A.A. ABED, Modified Vaginal Smear Cytology for the Determination of the Rat Estrous Cycle Phases, versus Ordinary Papanicolou Technique, Verified by Light and Scanning Electron Microscopic Examination of the Endometrium, 2007.
- A.P. Gupta, P. Singh, R. Garg, G.R. Valicherla, M. Riyazuddin, A.A. Syed, Z. Hossain, J.R. Gayen, Pancreastatin inhibitor activates AMPK pathway via GRP78 and ameliorates dexamethasone induced fatty liver disease in C57BL/6 mice, *Biomed. Pharmacother.* 116 (2019) 108959.
- A.A. Syed, M.I. Reza, M. Shafiq, S. Kumariya, P. Singh, A. Husain, K. Hanif, J.R. Gayen, Naringin ameliorates type 2 diabetes mellitus-induced steatohepatitis by inhibiting RAGE/NF- κ B mediated mitochondrial apoptosis, *Life Sci.* 257 (2020) 118118.
- W. Wang, X.Q. Ding, T.T. Gu, L. Song, J.M. Li, Q.C. Xue, L.D. Kong, Pterostilbene and allopurinol reduce fructose-induced podocyte oxidative stress and inflammation via microRNA-377, *Free Radic. Biol. Med.* 83 (2015) 214–226.
- X. Zhang, J.H. Zhang, X.Y. Chen, Q.H. Hu, M.X. Wang, R. Jin, Q.Y. Zhang, W. Wang, R. Wang, L.-L. Kang, Reactive oxygen species-induced TXNIP drives fructose-mediated hepatic inflammation and lipid accumulation through NLRP3 inflammasome activation, *Antioxid. Redox Signal.* 22 (2015) 848–870.
- M. el Amine Benarbia, D. Macherel, S. Faure, C. Jacques, R. Andriantsitohaina, Y. Malthiery, Plasmatic concentration of organochlorine lindane acts as metabolic disruptors in HepG2 liver cell line by inducing mitochondrial disorder, *Toxicol. Appl. Pharmacol.* 272 (2013) 325–334.
- M. Li, L. Xie, Y. Li, J. Liu, G. Nie, H. Yang, Synergistic effect of Huyang Yangkun Formula and embryonic stem cells on 4-vinylcyclohexene diepoxide induced premature ovarian insufficiency in mice, *Chin. Med.* 15 (2020) 1–14.
- Y. Goyal, K. Chugh, Y. Agrawal, Association of serum glutamic pyruvic transaminase and non-alcoholic fatty liver disease in controlled and uncontrolled diabetes, *J. Heal. Spec.* 2 (2014) 169.
- K.W. Ter Horst, M.J. Serlie, Fructose consumption, lipogenesis, and non-alcoholic fatty liver disease, *Nutrients* 9 (2017) 981.
- Y. Li, S. Xu, A. Giles, K. Nakamura, J.W. Lee, X. Hou, G. Donmez, J. Li, Z. Luo, K. Walsh, Hepatic overexpression of SIRT1 in mice attenuates endoplasmic reticulum stress and insulin resistance in the liver, *FASEB J.* 25 (2011) 1664–1679.
- W. Li, Y. Li, Q. Wang, Y. Yang, Crude extracts from *Lycium barbarum* suppress SREBP-1c expression and prevent diet-induced fatty liver through AMPK activation, *BioMed Res. Int.* 2014 (2014).
- B. Guo, Z. Li, Endoplasmic reticulum stress in hepatic steatosis and inflammatory bowel diseases, *Front. Genet.* 5 (2014) 242.
- R.J. Kaufman, Stress signaling from the lumen of the endoplasmic reticulum: coordination of gene transcriptional and translational controls, *Genes Dev.* 13 (1999) 1211–1233.
- D. Ron, P. Walter, Signal integration in the endoplasmic reticulum unfolded protein response, *Nat. Rev. Mol. Cell Biol.* 8 (2007) 519–529.
- L. Yang, P. Li, S. Fu, E.S. Calay, G.S. Hotamisligil, Defective hepatic autophagy in obesity promotes ER stress and causes insulin resistance, *Cell Metabol.* 11 (2010) 467–478.
- L. Zhou, F. Liu, Autophagy: roles in obesity-induced ER stress and adiponectin downregulation in adipocytes, *Autophagy* 6 (2010) 1196–1197.
- M.J. Romero-Aleshire, M.K. Diamond-Stanic, A.H. Hasty, P.B. Hoyer, H.L. Brooks, Loss of ovarian function in the VCD mouse-model of menopause leads to insulin resistance and a rapid progression into the metabolic syndrome, *Am. J. Physiol. Integr. Comp. Physiol.* 297 (2009) R587–R592.
- J.C. Lohff, P.J. Christian, S.L. Marion, A. Arrandale, P.B. Hoyer, Characterization of cyclicity and hormonal profile with impending ovarian failure in a novel

- chemical-induced mouse model of perimenopause, *Comp. Med.* 55 (2005) 523–527.
- [43] C.M. Elks, J.D. Terrebonne, D.K. Ingram, J.M. Stephens, Blueberries improve glucose tolerance without altering body composition in obese postmenopausal mice, *Obesity* 23 (2015) 573–580.
- [44] D.G. Sudhanshu, Assessment of liver damage in male albino rats after repetitive heat stress of moderate level, *Natl. J. Physiol. Pharm. Pharmacol.* 3 (2013) 147–152.
- [45] I.-S. Hwang, H. Ho, B.B. Hoffman, G.M. Reaven, Fructose-induced insulin resistance and hypertension in rats, *Hypertension* 10 (1987) 512–516.
- [46] T.A. Tobey, C.E. Mondon, I. Zavaroni, G.M. Reaven, Mechanism of insulin resistance in fructose-fed rats, *Metabolism* 31 (1982) 608–612.
- [47] H.L. Kammoun, H. Chabanon, I. Hainault, S. Luquet, C. Magnan, T. Koike, P. Ferré, F. Fougère, GRP78 expression inhibits insulin and ER stress-induced SREBP-1c activation and reduces hepatic steatosis in mice, *J. Clin. Invest.* 119 (2009) 1201–1215.
- [48] H. Yin, M. Hu, X. Liang, J.M. Ajmo, X. Li, R. Bataller, G. Odena, S.M. Stevens Jr., M. You, Deletion of SIRT1 from hepatocytes in mice disrupts lipin-1 signaling and aggravates alcoholic fatty liver, *Gastroenterology* 146 (2014) 801–811.
- [49] C. Zhang, X. Chen, R.M. Zhu, Y. Zhang, T. Yu, H. Wang, H. Zhao, M. Zhao, Y.L. Ji, Y.H. Chen, X.H. Meng, W. Wei, D.X. Xu, Endoplasmic reticulum stress is involved in hepatic SREBP-1c activation and lipid accumulation in fructose-fed mice, *Toxicol. Lett.* 212 (2012) 229–240.
- [50] X. Li, Z. Xu, S. Wang, H. Guo, S. Dong, T. Wang, L. Zhang, Z. Jiang, Emodin ameliorates hepatic steatosis through endoplasmic reticulum–stress sterol regulatory element-binding protein 1c pathway in liquid fructose-feeding rats, *Hepatol. Res.* 46 (2016) E105–E117.
- [51] Z. Zheng, C. Zhang, K. Zhang, Role of unfolded protein response in lipogenesis, *World J. Hepatol.* 2 (2010) 203.
- [52] L.P. Ren, S.M.H. Chan, X.Y. Zeng, D.R. Laybutt, T.J. Iseli, R.Q. Sun, E.W. Kraegen, G.J. Cooney, N. Turner, J.-M. Ye, Differing endoplasmic reticulum stress response to excess lipogenesis versus lipid oversupply in relation to hepatic steatosis and insulin resistance, *PLoS One* 7 (2012) 30816.
- [53] S.M.H. Chan, R.Q. Sun, X.Y. Zeng, Z.H. Choong, H. Wang, M.J. Watt, J.M. Ye, Activation of PPAR α ameliorates hepatic insulin resistance and steatosis in high fructose-fed mice despite increased endoplasmic reticulum stress, *Diabetes* 62 (2013) 2095–2105.
- [54] J. Han, R.J. Kaufman, The role of ER stress in lipid metabolism and lipotoxicity, *J. Lipid Res.* 57 (2016) 1329–1338.
- [55] D.S. Kim, S.K. Jeong, H.R. Kim, D.S. Kim, S.W. Chae, H.J. Chae, Metformin regulates palmitate-induced apoptosis and ER stress response in HepG2 liver cells, *Immunopharmacol. Immunotoxicol.* 32 (2010) 251–257.
- [56] W.G. Choi, J. Han, J.H. Kim, M.J. Kim, J.W. Park, B. Song, H.J. Cha, H.-S. Choi, H.T. Chung, I.K. Lee, T.S. Park, M. Hatzoglou, H.S. Choi, H.J. Yoo, R.J. Kaufman, S.H. Back, eIF2 α phosphorylation is required to prevent hepatocyte death and liver fibrosis in mice challenged with a high fructose diet, *Nutr. Metab. (Lond.)* 14 (2017) 48.